Dynamic photovoltaic greenhouse: Energy balance in completely clear sky condition during the hot period

Alvaro Marucci*, Andrea Cappuccini

DAFNE, University of Tuscia, Via San Camillo de Lellis s.n.c., 01100 Viterbo, Italy

Abstract

In this study, the energy balance for a prototype dynamic photovoltaic greenhouse was determined for days with completely clear skies during the summer. The rotation of photovoltaic panels along the longitudinal axis was the unique feature of the prototype. Inside the greenhouse, the degree of shading most suitable for the requirements of the crop, the cultivation period, the latitude of the site and the climatic conditions was selected by the rotation of the panels. To avoid energy losses from the reflection caused by unfavourably positioned photovoltaic panels, the panels were provided with highly reflective aluminium mirrors.

To evaluate the possibility of using the dynamic photovoltaic greenhouse prototype as a passive cooling system, the energy balance was determined. Based on the results, the use of photovoltaic elements offers an alternative perspective for both the shading of greenhouses and the production of electricity in periods of heat and in areas with a warm climate.

With planning that considers the type of crop, geographic coordinates, length of the cultivation period and local weather conditions, the use of this structure can reconcile agricultural production with the production of energy from renewable sources.

Nomenclature

Alphabetic symbols

R	global solar radiation [W m^{-2}]
RT	heat transfer due to radiation [W m^{-2}]
T	heat transfer due to transmission [W m^{-2}]
E_V	heat transfer due to ventilation [W m^{-2}]
n	Julian day
K	thermal transmittance (W m^{-2} °C^{-1})
V	flow rate of ventilation (Kg Dry Air h^{-1})
H	enthalpy (KJ Kg Dry Air^{-1})
x	weight of water vapour in air (Kg water Kg Dry Air^{-1})
p	pressure (Pa)
f	view factor
h	hour days
A	altitude (km)
C_d	diffusivity coefficient of the cover
S	thickness of the cover
n	refractive index
k	absorption coefficient
r	surface reflectance

Subscripts

e	external
re	reflected external
i	internal
ri	reflected internal
b	direct
d	diffuse
c	cover
rg	reflected from the ground
ag	absorbed by the ground
ac	absorbed by the cover
g	ground
ia	internal air
atm	atmosphere
sky	vault of heaven

Greek letters

ω	solar hour angle (°)
δ	declination angle (°)
α	solar altitude angle (°)
θ_i	solar incidence angle (°)
θ_z	solar zenith angle (°)
ν	angle between the horizontal projection of the surface normal and the direction south (°)
φ	latitude of the location (°)
σ	Stefan–Boltzmann constant (W m^{-2} K^{-4})
ε_{12}	emissivity
τ	transmittance
ρ	cover reflectance
α_c	absorbance

1. Introduction

In recent years, cultivation in greenhouses has expanded worldwide [1] because of the high level of production obtained in these structures compared with production in the field [2].

With control of the internal greenhouse environment, production increases because the greenhouse is almost independent of the external weather conditions. Additionally, the microclimate inside the structure can be programmed through simulation models to meet the cultivation requirements.

Models that predict the microclimate inside a greenhouse are a fundamental tool used by farmers to manage the production cycle of a crop and by designers to provide improvements in climatic control systems [3].

Inside the greenhouse, the microclimatic parameters of air temperature [4], relative humidity [5], level of light [6] and concentration of CO2 [7] affect not only the quality and productivity of the cultivated crop [8,9] but are also critical factors that affect the spread of pathogens and diseases [10]. Furthermore, with the control of these parameters compared with external conditions, farmers can increase or decrease the cultivation time to increase the economic competitiveness of the farm.

In the first research to analyse the energy balance in greenhouses [11e13], the focus was on the thermal behaviour of the structure. Subsequently, many models of energy balance were developed to understand the relationships between internal microclimatic parameters and external climatic and some construction parameters (e.g., section shape and covering material, among others) [14e23].

Simulation models are widely used to predict greenhouse environments because these models are faster, cheaper and more flexible than the predictions based on experiments [3,24].

The characterization of the energy balance for a greenhouse in each bioclimatic zone of the world is fundamental to assess the feasibility of the system and to improve the control of the internal microclimate. Moreover, the construction characteristics of the structure and the mechanical systems for microclimatic control are significantly affected by geographical factors such as latitude. In the countries of northern and central Europe, which are characterized by cold winters and low levels of solar radiation [1],

Venlo greenhouses have been developed almost exclusively. In these countries, greenhouses must minimize the loss of heat through the use of glass and a favourable volume: surface ratio, in addition to exploiting most of the diffuse radiation with eaves high in the structures.

By contrast, the requirements of greenhouses for regions of the Mediterranean are the opposite; in these regions, the “Mediterranean greenhouse” is used, with a large spread of plastic for a covering material (providing cover for over 90% of the floor area).

The energy used to create favourable microclimatic conditions is contributed primarily by solar energy. Externally supplied energy is used only during short cold periods (mostly at night) [25,26] and when the plants must be protected from excessive heat by lowering the temperature [27]. In some periods, lower temperatures are necessary because the intensity of solar radiation reaching the surface of the earth exceeds the requirements of crops and increases the internal air temperature to intolerable levels [28,29].

Although the protection of plants from intense solar radiation is relatively easy with shading [30], the protection from high air temperatures is difficult to achieve with only natural ventilation [31].

To prevent excessive internal air temperatures, ventilation with cooled air (e.g., evaporative filters, and others), use of water mist or complete opening of the cover (sky system) is required. However, for all these remedies to control high temperatures, external energy is required, with a significant increase in production costs.

Therefore, in this study, the energy balance of a prototype dynamic photovoltaic greenhouse with different degrees of shading during days in the summer with clear skies was evaluated. For the Mediterranean latitudes, these conditions are the most critical in the evaluation of a greenhouse.

The cover of the structure that faced south was covered with photovoltaic panels. The panels were rotated along the longitudinal axis to adjust the shading inside the greenhouse, and the different degrees of shading were caused by the projection of shade from the panels inside the greenhouse. With this arrangement, it may be possible to balance the production of photovoltaic energy with that of agriculture.
In studies of the photovoltaic greenhouse, a degree of shading that was fixed too high reduced the growth, development and productivity of the crops, whereas a degree of shading that was fixed too low substantially reduced the production of electrical energy. With the analysis of the energy balance, the possibility of using the dynamic photovoltaic greenhouse as a passive cooling system and simultaneously producing energy from renewable sources was assessed.
The following percentages of shading were analysed:

- 0%;
- 10%;
- 20%;
- 30%;
- 40%;
- 50%;
- 60%;
- 70%;
- 75%;
- 78%.

The zero percent shade referred to the shade caused by the thickness of the photovoltaic panels (3%). The maximum shading was 78% because of the spacing of the photovoltaic modules, which allowed 22% of the solar radiation to enter the greenhouse when the panels were parallel to the cover.
Furthermore, the shading was measured on each date at 12:00 p.m.; because the degree of shading changed continuously during the day, standardizing the time of measurement avoided continuously moving the panels to maintain the degree of shading.
Based on previous studies with photovoltaic greenhouses, the use of photovoltaic panels as a covering material for greenhouses was analysed only with the panels in a static position, which is an approach that neglects agricultural production in favour of photovoltaic production. Silicon panels (i.e. monocrystalline or twin-Si) are mostly used and present the highest values of efficiency (17e18%) [32].
Because the angle of a panel affects the angle of incidence of the rays of the sun on the panel, the tilt angle of a photovoltaic system is one of the most important factors to maximize the conversion of solar energy [33]. Generally, in the design of solar systems, the optimal angle is determined to target the optimum production of energy [34].
Worldwide, many studies have focused on the optimal tilt angle of the photovoltaic panels (Turkey [35,36], Illinois (USA) [37], Syria [38], Cyprus [39], China [40], Saudi Arabia [41], Spain [42], Australia [43], and Serbia [44]). Additionally, numerous studies use an equation to calculate the optimal tilt angle of the photovoltaic panels. Some of the equations are simple and use latitude as a function (φ): φ ± 15° [45]; φ e 10° [46]; 0.9 φ [47]; and 0.917 φ + þ 0.321 [48]. However, other equations are the result of more complex correlations [49 e 51] that use several constants determined for each month or each season.

With agricultural production as the primary objective of greenhouse operation, we propose a new system that uses the rotation of photovoltaic panels and highly reflective aluminium mirrors to potentially combine the production of agriculture with that of energy.
Furthermore, the energy balance was analysed to determine the energy flows of this structure. We then studied the possible use of this structure as a passive cooling system with analyses of different degrees of internal shading and consideration of parameters such as the type of crop, day of the year, solar geometry, external climatic conditions and geographic coordinates.
The innovations of this paper can be summarized as follows: (1)
Achieving a variable shading level of greenhouse coverage. The shading will be adjusted depending on the weather conditions and crops requirements, including the cultivation period, the type of crop and the parameters that influence the solar radiation, such as the time of day, day of the year, latitude, altitude and degree of sky coverage. The photovoltaic greenhouses implemented so far exhibit fixed shadings degrees, which if they become too high, can reduce the growth and development of the crops and productivity. On the other hand, if they are too small, they can reduce the electricity production. (2) Striking a balance between photovoltaic energy production and agricultural production on the same land unit, with the aim of optimizing the economic productivity of this mixed system. (3) Significantly reducing losses by reflection of the photovoltaic panels, which, to reduce shading, will need to have a non-optimal tilt angle. The reflected solar energy will be almost completely recovered, thanks to the presence of highly reflective mirrors, which are made of aluminium and aligned to the rays of the sun. (4) Installing a photovoltaic surface on nearly 100% of the roof area and reducing the projection of the panels on the ground through the rotation of the photovoltaic panels upwards to remove the shading and thereby allow the greatest flexibility in the total use of the structure.
Based on this background, the paper is organized as follows. In Section 2, the prototype is described, and the calculations for the inclination of the photovoltaic panels and for the energy balance model are presented. In Sections 3 and 4, the results of the energy balance calculations are presented followed by related discussions and conclusions, respectively.

2. Materials and methods

2.1. Description of the prototype

The prototype of the dynamic photovoltaic greenhouse is on the “N. Lupori” didactic experimental farm of Tuscia University (Viterbo, Lazio, Italy; 42°25’38’’ N, 12°04’51’’ E; 306 m in altitude).
The greenhouse was constructed of iron and glass with a polycarbonate transverse wall and was asymmetrical in cross section in the eastewest orientation (EeW). The shape of the section with the photovoltaic modules was specifically designed to facilitate the production of energy, and this flap that faced south had the largest surface area with the optimum tilt angle for the latitude of the site (Fig. 1).
In Table 1, the geometric characteristics of the prototype are presented.
The pitch that faced towards the south was covered with 24 polycrystalline photovoltaic panels (SYM 30P-7V, Sunenergy. Zol lino, Lecce, Italy). The panel dimensions were 1200 mm x 20 mm.
The system was composed of three strings of 8 panels each that were connected in series.
Each string had a manual system for rotation of the panels along the longitudinal axis. The rotation of the panels adjusted the amount of shade inside the structure. The primary problem with this rotation system was the possible loss of solar radiation through reflection; this problem occurred because the inclination of the photovoltaic panels differed from the angle that was optimal to

capture solar radiation. Also, shading 50% of a PV single-cell, the power production of the PV module is reducing by more than 30% [52]. To overcome this drawback, the photovoltaic panels were provided with 24 highly reflective aluminium mirrors (98%) (Vega Energy SP, Almeco group, San Giuliano Milanese, Milano, Italy). The mirrors also had a manual system for rotation along the longitudinal axis (Fig. 2).
For mechanical ventilation, a fan (1000 m^3 h^{-1}) was positioned on the west transverse wall with an aluminium grid on the opposite transverse wall. Additionally, there were six openings for natural ventilation (three on the south vertical wall and three on the north pitch). The fan was connected to a thermostat, and when the internal air temperature exceeded 26 °C, the fan was turned on.
To determine the degree of shadowing, the ratio of the length of the projection of the panels, which included the frame (21 cm), on the pitch and the distance from the rotation point of the panels (27 cm) was used. When the modules were parallel to the pitch, the maximum degree of shadowing was reached at 78%. To reduce the degree of shadowing, the rotation of the panels from the longitudinal side reduced the projection of the shadow on the pitch.
Four sensors (thermohygrometer CS215 þ CS300 pyranometer) were used to record the climatic parameters both inside and outside (air temperature, relative humidity and solar radiation on the horizontal plane) the greenhouse, with 3 sensors (S1, S2 and S4) positioned internally and 1 placed outside the structure (S3).
The current and voltage values of the sensors were as follow:

- CE-IZ04-35A2-1.0/0-50A DC Current Transducer (Phidgets, Canada);
- CE-VZ02-32MS1-0.5 DC Voltage Sensor 0e200 V (Phidgets, Canada).

Experimental measurements are all associated with uncertainty, and therefore, error analysis is crucial to determine the accuracy and deviation of calculated values from the actual values in an experiment. In this work, the errors were primarily related to sensitivity of the instruments and inaccurate measurements.
Moreover, the temperature, relative humidity and solar radiation sensors recorded measurements at different positions. In Table 2, a detailed listing of the levels of uncertainty associated with the sensors is presented.
The sensors were connected to a Campbell CR 1000 data acquisition system (Accuracy of ±0.06% of reading þ offset, at 0° e40 °C), which recorded values at intervals of 15 min.
To avoid shading inside the greenhouse and on the photovoltaic cells, the highly reflective mirrors were always oriented according to the solar rays.
The following percentages of shading were examined:

- 0%;
- 10%;
- 20%;
- 30%;
- 40%;
- 50%;
- 60%;
- 70%;
- 75%;
- 78%.

Because the sun is at the maximum height (Fig. 3) and is defined by Eqs. (1)e(12), in this study, the inclination of the panels was calculated to obtain the percentages of shading at 12:00 p.m. for each date of the experiment. The inclination of the photovoltaic panels depended on the latitude, the Julian day, the time of day and consequently, on the position of the sun at different times of the day.

$$R_e = 1367 \times \left[1 + 0.033 \cos\left(\frac{360}{365} \times n\right)\right] \quad (1)$$

$$A_0 = \left[0.4237 - 0.00821(6 - A)^2\right] \left[1 + 0.03 \sin\left(\pi \frac{91 + n}{182}\right)\right] \quad (2)$$

$$A_1 = \left[0.5055 - 0.00595(6.5 - A)^2\right] \left[1 + 0.01 \sin\left(\pi \frac{91 + n}{182}\right)\right] \quad (3)$$

$$K = \left[0.2711 - 0.01858(2.5 - A)^2\right] \left[1.01 + 0.01 \sin\left(\pi \frac{91 + n}{182}\right)\right] \quad (4)$$

$$\omega = \frac{360}{24}(12 - h) \quad (5)$$

$$\delta = 23.45 \sin\left[\frac{360}{365}(284 + n)\right] \quad (6)$$

$$\alpha = \sin^{-1}(\sin\varphi \sin\delta + \cos\varphi \cos\delta \cos\omega) \quad (7)$$

$$\psi = \alpha + \textit{Photovoltaic pitch slope}\ (33^\circ) \quad (8)$$

$$X = 0.27 \times \textit{shade} \quad (9)$$

$$\varepsilon = 180 - \psi \quad (10)$$

$$\gamma = \sin^{-1}\left(X \times \frac{\sin\varepsilon}{0.21}\right) \quad (11)$$

$$\beta = 180 - (\varepsilon + \gamma) \quad (12)$$

2.2. Energy balance of the prototype of a dynamic photovoltaic greenhouse

In the determination of the energy balance, the different energy flows were calculated (Fig. 4): The energy balance equation (13) was as follows:

$$R_i = RT_{g,sky} + RT_{g,atm} + RT_{c,sky} + RT_{c,atm} + T + V \quad (13)$$

The global solar radiation R_i (direct and diffuse radiation) in side the greenhouse under clear sky conditions was calculated using Eq. (14):

$$R_i = R_e[\tau_b(1 + C_d) + \tau_d]\cos\theta_i\tau_c \quad (14)$$

where Re is the extraterrestrial solar radiation in W m^{-2}, τ_b is the transmissivity of the atmosphere to the direct radiation, C_d is the diffusivity coefficient of the cover, τ_d is the transmissivity of the atmosphere to the diffuse radiation, ϑ_i is the solar incidence angle and τ_c is the transmissivity of the cover and the walls to solar radiation.
The solar incidence angle (ϑi) was defined with Eq. (15):

$$\begin{aligned}\vartheta_i = \sin^{-1}(&\sin\varphi\sin\delta\cos\vartheta_z - \cos\varphi\sin\delta\sin\vartheta_z\cos\nu \\ &+ \cos\varphi\cos\delta\cos\omega\cos\vartheta_z + \sin\varphi\cos\delta\cos\omega\sin\vartheta_z\cos\nu \\ &+ \cos\delta\sin\omega\sin\vartheta_z\sin\nu)\end{aligned} \quad (15)$$

The transmissivity of the atmosphere to the direct radiation (τ_b) was defined with Eq. (16):

$$\tau_b = A_0 + A_1 e^{\frac{-K}{\cos\theta_z}} \quad (16)$$

where A0, A1 and K are dimensionless coefficients defined by Eqs. (2)e(4).
The transmissivity of the atmosphere to the diffuse radiation (td) was defined with Eq. (17):

$$\tau_d = 0.271 - 0.294\tau_b \quad (17)$$

The transmissivity (tc) of the cover and the walls to solar radi ation was determined using a model reported in the literature [53].
Heat transfer due to transmission (W m2) from the walls and the cover was calculated with Eq. (18):

$$T = KS(t_i - t_e) \quad (18)$$

K = thermal transmittance (W m^{-2} °C^{-1});
S = surface (m^2);
t_i = internal temperature (°C);
t_e = external temperature (°C).

The heat transfer due to ventilation (W m2); was calculated with Eq. (19):

$$E_v = V(H_i - H_e) \quad (19)$$

E_v = heat transfer due to ventilation (W m^{-2});

V = flow rate of ventilation (Kg Dry Air h^{-1});
H_i = internal air enthalpy (KJ Kg Dry Air^{-1});
H_e = external air enthalpy (KJ Kg Dry Air^{-1}).

The enthalpy H (KJ Kg Dry Air^{-1}) of a Kg of air at temperature t (°C) with water content equal to x (Kg water Kg Dry Air^{-1}) was obtained with Eq. (20):

$$H = 1.005t + x(2499.5 + 2.005t) \quad (20)$$

The value x (Kg water Kg Dry Air1) is the weight of water vapour in air and was determined from a psychrometric diagram or with the following Eq. (21):

$$x = 0.6215 \frac{p_{H_2O}}{p - p_{H_2O}} \quad (21)$$

where p ¼ atmospheric pressure (Pa); and pH2 O ¼ vapour pressure of the air, expressed in Pa at temperature T (————————————K) and relative humidity UR (%). The pH2 O was obtained with Eq. (22);

$$p_{H_2O} = 1.41 \times 10^{10} e^{\frac{-3928.5}{T-41.5}} \times UR \quad (22)$$

The heat transfer due to radiation (W m2) was calculated using Eq. (23):

$$RT_{1,2} = \varepsilon_{12} f_{12} \sigma \left(T_1^4 - T_2^4\right) \quad (23)$$

RT_{12} = heat transfer due to radiation (W m^{-2});
σ = Stefan–Boltzmann constant (W m^{-2} K^{-4});
ε_{12} = emissivity;
f = view factor; T = absolute temperature (°K).

3. Results and discussion

The averages and the minimum and maximum values of the microclimatic parameters recorded outside and inside the structure on the dates of the experiment with the percentages of shading are shown in Table 3.

As shown in Fig. 5, the air temperatures inside the greenhouse followed the trend of air temperatures outside the structure. During the experiment, the dates examined were characterized by completely clear skies. The maximum external air temperature did not exceed the threshold value of 32 °C, whereas the respective internal temperatures exceeded this limit on all dates, with the maximum value recorded on 29th August (45.3 °C). The difference in air temperature between the inside and outside of the greenhouse ranged from 10 °C to 20 °C during the middle of the day, whereas at night, the range was between 2 °C and 5 °C.

For the relative humidity (Fig. 6) recorded outside the greenhouse, on three days (10th August, 9th September and 28th September), the air saturation average values were between 55% and 85%. Inside the prototype greenhouse, the maximum value recorded was 91.7% (9th September), with average values that ranged from 45% to 70%.

The trends in the intensity of global solar radiation on a horizontal plane (W m^{-2}) registered inside and outside the structure are shown in Fig. 7.

The maximum global solar radiation outside the greenhouse ranged between 700 and 950 W m^{-2}.

The range of global solar radiation recorded inside the structure was much larger than that outside the structure (100e950 W m^{-2}). The wider range occurred because of the different inclinations of the photovoltaic panels used to obtain different degrees of shading, which were more or less correlated with a consequent decrease in the internal radiation. The dates of the experiment reported in Fig. 7 are listed in ascending order of the percentage of shading.

The values for solar radiation outside and inside and the total energy losses from the greenhouse (i.e., ventilation, radiation and transmission) are shown in Fig. 8.

The ratio of the internal and external solar radiation was not consistent with the degree of shading established because the shading percentage referred to the solar radiation that passed through the structure from the photovoltaic roof and excluded the portion that passed through the vertical walls.

On the dates when the percentage shading was less than 70%, the solar radiation available inside the structure always exceeded 10 MJ m 2. The maximum value (27.1 MJ m^{-2}) was recorded on the date in which the percentage of shading was zero (17th August).

With shading greater than 70%, the internal solar radiation fell slightly below the threshold of 10 MJ m^{-2}.

When the percentage of shading was below 30%, the energy available in the structure approached 20 MJ m 2 or exceeded this value (17th August), which is a value that greatly exceeded the requirements of the most demanding vegetable crops.

The actual energy balance and therefore the net energy that remained inside the greenhouse (positive values) is shown in Fig. 9. Positive values (17th August, 28th September and 3rd October) indicated that the energy inside the photovoltaic structure exceeded the requirements; therefore, the shading caused by the panels could be increased as a passive protection system. Negative values (29th August, 9th September and 10th August) indicated that the greenhouse required an increase in energy because of excessive shading caused by the photovoltaic panels.

The total energy losses and the trends for the losses from individual flows (i.e., transmission, radiation and ventilation) are shown in Fig. 10. Based on the trend for the individual losses on the dates of the experiment, the ventilation caused a large loss of energy. Because the experiment was performed during the summer, we expect similar losses to occur at high temperatures generally.

The energy lost through ventilation decreased during the experiment, which was consistent with the decrease in air temperature. The fan was connected to a thermostat that activated the fan at a threshold of 26 ▪C internal air temperature. The energy lost by ventilation flow was recorded during the middle of the day, with the relative maximum flows between 200 and 300 W m^{-2}, except for the final two days of the trial (3rd and 5th October).

The energy lost by transmission referred to the flows from boththe glass structure and the polycarbonate wall. These flows were greatly affected by the temperature differences between the external and internal environments, and as expected, the energy lost through transmission was directly proportional to the temperature difference. The maximum values of transmission loss were registered during the middle of the day when the differences in air temperature were the greatest and were between 60 and 160 W m^{-2}.

The energy losses through radiation were strongly affected by the covering material and in particular, by the opacity of the cover to the far infrared portion of the spectrum. Because the glass was opaque to this wavelength, the energy was absorbed and reemitted through radiation. In this study, plants were absent inside the structure, and only the losses through radiation from the cover material and from the ground were considered. The sum of these losses through radiation generated a maximum output of power between 50 and 100 W m^{-2} in the central hours of each day of testing. The losses through radiation were also affected by the shielding action of the photovoltaic panels, particularly when the panels were positioned for a high percentage of shading (>60%).

The values for the total energy lost and the components of the loss (MJ m^{-2}) are shown in Fig. 11. An increase in the degree of shading resulted in a decrease in the temperature difference between the external and internal environments, which led to a decrease in the losses caused by ventilation. However, the proportion of ventilation to the total losses showed an upward trend, and with

shading of 0%, the losses from ventilation were 38% of the total, but with 78% shading, the percentage lost increased to 67%.
The percentage of energy lost through transmission was constant throughout the experiment, ranging between 20% and 30% of the total losses.
The energy lost by radiation was strongly affected by the conditions of the greenhouse, and the shielding action of the panels had a strong effect on those losses. For shading percentages less than 40%, the energy lost through radiation was between 35% and 20% of the total loss, with the effect decreasing as shading increased. For shading over 40%, the percentage lost through radiation continued to decrease until the loss was 4%.
The photovoltaic production and the outside solar radiation (MJ m^{-2}) are shown in Fig. 12. The maximum values for photovoltaic
energy (2.4 MJ m^{-2}) were obtained when the shading percentage was high (78%) and the tilt angle of the panels was coincident with that of the photovoltaic roof (β = 30°).
When the solar panels were positioned horizontally (β = 0°, 9th September), the energy produced was reduced by approximately 30%. For low levels of shading (0%, 10%, 20%, 30%) the photovoltaic cells were exposed to the north (β < 0°, with a consequent decrease in the production of energy.
Based on the results, the use of photovoltaic elements to shade greenhouses and to simultaneously produce electricity with the energy surplus that exceeds the requirements of crops, particularly in periods of heat and in areas with a warmer climate, was demonstrated. With the analysis of the energy balance, it was possible to evaluate the use of the prototype of a dynamic photovoltaic greenhouse as a passive cooling system.
When compared with the energy requirements of most horticultural crops [54e58], the amount of energy available inside the structure on each date of the experiment was more than sufficient for the normal development of agriculture.
On some dates of the experiment, the solar energy available inside the structure exceeded the solar energy recorded outside the greenhouse and the solar energy required for the normal physiological activity of most crops. Therefore, with planning that considers the type of crop, geographic coordinates, length of the cultivation period and local weather conditions, the use of this structure to reconcile agricultural production with the production of renewable energy is possible.
The advantage in the rotation of the photovoltaic panels is that the degree of shading most suitable to meet the requirements of the crop, cultivation period, and type of crop can be determined, and the determination includes incorporation of the parameters that influence solar radiation such as the day of the year, time of day, latitude, altitude and coverage of the sky.

3.1. Economic considerations

The incentive rate of the “Feed-in Tariff” reduces the payback time required for a PV system [59e63] and is adopted in many European countries. Although the amount of public subsidies is declining, when subsidies are assigned, they are guaranteed for 20 years. Assuming a constant optimum tilt angle o throughout the year, the yearly sum of solar electricity generated by a 1 kWp system is equal to 1.400 kWh kWp^{-1} [64,65], and the energy production of the PV system was 1120 kWh, which is equivalent to137.4 kWh m^{-2} $year^{-1}$.
Article 5, paragraph 3 of Decree 5 July 2012 reports that “…installations whose modules are structural components of pergolas, greenhouses, acoustic fences, shelters and platform roofs are entitled to a tariff equal to the average between the tariff due to «PV Plants built over buildings» and the tariff due to «other PV plants»” [66].
The annual incentive income, derived from the feed-in tariff system (0.327 VkWh 1), was 366.24 Vfor all the PV energy produced, regardless of the final use of the electricity (consumption or sale).

Moreover, income was also indirectly generated through consumption of energy that did not require purchase, which amounted to V201.6 (average electricity price: V0.18 kWh 1) [54].
For the photovoltaic system and the handling system of this prototype, the overall cost was 3500 V.

4. Conclusions

In this study, we proposed the use of a photovoltaic greenhouse as an innovative solution to reconcile the production of electricity by photovoltaic panels with that of agriculture. With analysis of the components of the energy balance, the possibility of using the prototype of the dynamic photovoltaic greenhouse as a passive cooling system was assessed. The results of this study were based on the latitude of the structure and on specific conditions such as days with completely clear skies and the absence of plants inside the greenhouse.
With information on parameters such as the physiological requirements for crop production, geographical coordinates, time of year and local climatic conditions of the site, the most appropriate percentage of shading can be selected. For example, the results for the final two dates of the experiment (3rd and 5th October) were obtained with a high degree of shading (75% and 78%), and it is advisable to use these percentages of shading for periods in which the intensity of outside solar radiation is high (e.g., in the summer).
In future studies, the compatibility of the dynamic photovoltaic greenhouse will be assessed with plant species that have high light demands, particularly during seasons with low intensity solar radiation. Additionally, the production of energy using photovoltaic modules with a variable slope on days with partially or totally cloudy skies will be evaluated.

References

Table 1
Geometric characteristics of the prototype greenhouse.

Length	3.79 m
Width	2.41 m
Ridge height	2.05 m
Eave height (south wall)	0.94 m
Eave height (north wall)	1.36 m
Photovoltaic surface	8.15 m^2
Photovoltaic pitch slope (south)	30°
Non-photovoltaic pitch slope (north)	51°
Glass thickness	3 mm

Table 2
Accuracy of the sensors.

Sensors	Accuracy
Hygrometer	(at 25 °C): ±2% (10%–90% range); ±4% (0%–100% range)
Thermometer	±0.3 °C at 25 °C ±0.4 °C (+5 °C to +40 °C) ±2% (−40 °C to +70 °C)
Pyranometer	±5% for daily total radiation
DC current transducers	1%
DC voltage sensor	0.50%

Table 3
Averages and minimum and maximum values of the microclimatic parameters with shading percentages.

	Outside air temperature (°C)			Inside air temperature (°C)			Outside RH (%)			Inside RH (%)			External solar radiation (MJ m^{-2} d^{-1})	Internal solar radiation (MJ m^{-2} d^{-1})	Shading percentage (%)
	Min.	Max.	Mean	Min.	Max.	Mean	Min.	Max.	Mean	Min.	Max.	Mean			
August 10th	17.1	31.1	23.7	19	41.7	29.1	43.7	100	75.1	27.9	90.1	59.5	26.0	11.6	70
August 17th	13.9	29.4	21.1	15.1	42.4	27.3	27.5	86.8	58.1	15.3	74.6	45.6	26.9	27.1	0
August 29th	17.6	30.6	23.4	18.4	45.3	29.4	35.6	89.2	64.3	18.2	76.2	51.2	24.0	18.8	30
September 9th	15.9	28.3	21.3	17.5	39.4	26.4	52	100	84.4	30.5	91.7	67.4	21.5	12.0	60
September 13th	11.5	26.1	18	12.3	37.4	22.8	36	95.3	69.5	21.9	86.6	57.7	21.9	14.2	50
September 26th	11.9	24.4	17.4	12.4	36.3	22	39.7	95.9	65.7	21.4	89.2	55.2	19.7	19.6	10
September 27th	12.4	27.1	19	13.1	38.6	23.5	38.8	67.9	55	21.1	62.6	45.3	19.2	17.0	20
September 28th	13.9	27	19.5	14.8	36.4	23.6	37	100	67.4	23.8	87	55.8	19.1	14.1	40
October 3rd	14.1	25.9	18.6	14.5	33	21.8	47.9	90.7	73.3	33.4	86.4	62.8	17.0	8.8	75
October 5th	12.8	25.3	17.6	13.3	32.8	21	41	94.1	75.8	29.9	88	64.7	17.2	7.6	78

Fig. 1. Asymmetrical cross section of a prototype dynamic photovoltaic greenhouse.

Fig. 2. Prototype of dynamic photovoltaic greenhouse.

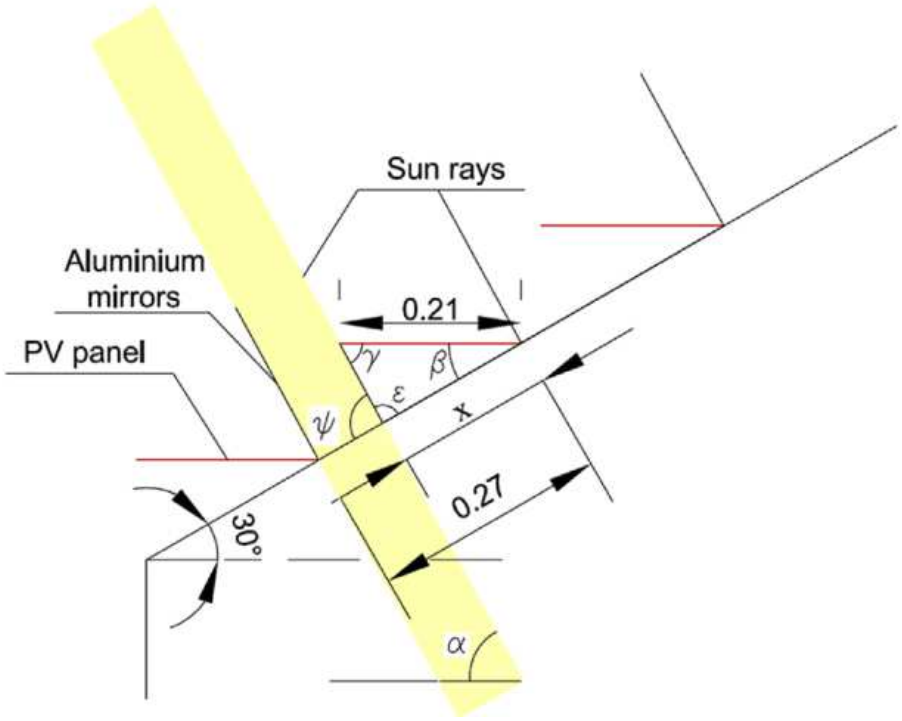

Fig. 3. Scheme for the values to calculate the inclination of the photovoltaic panels.

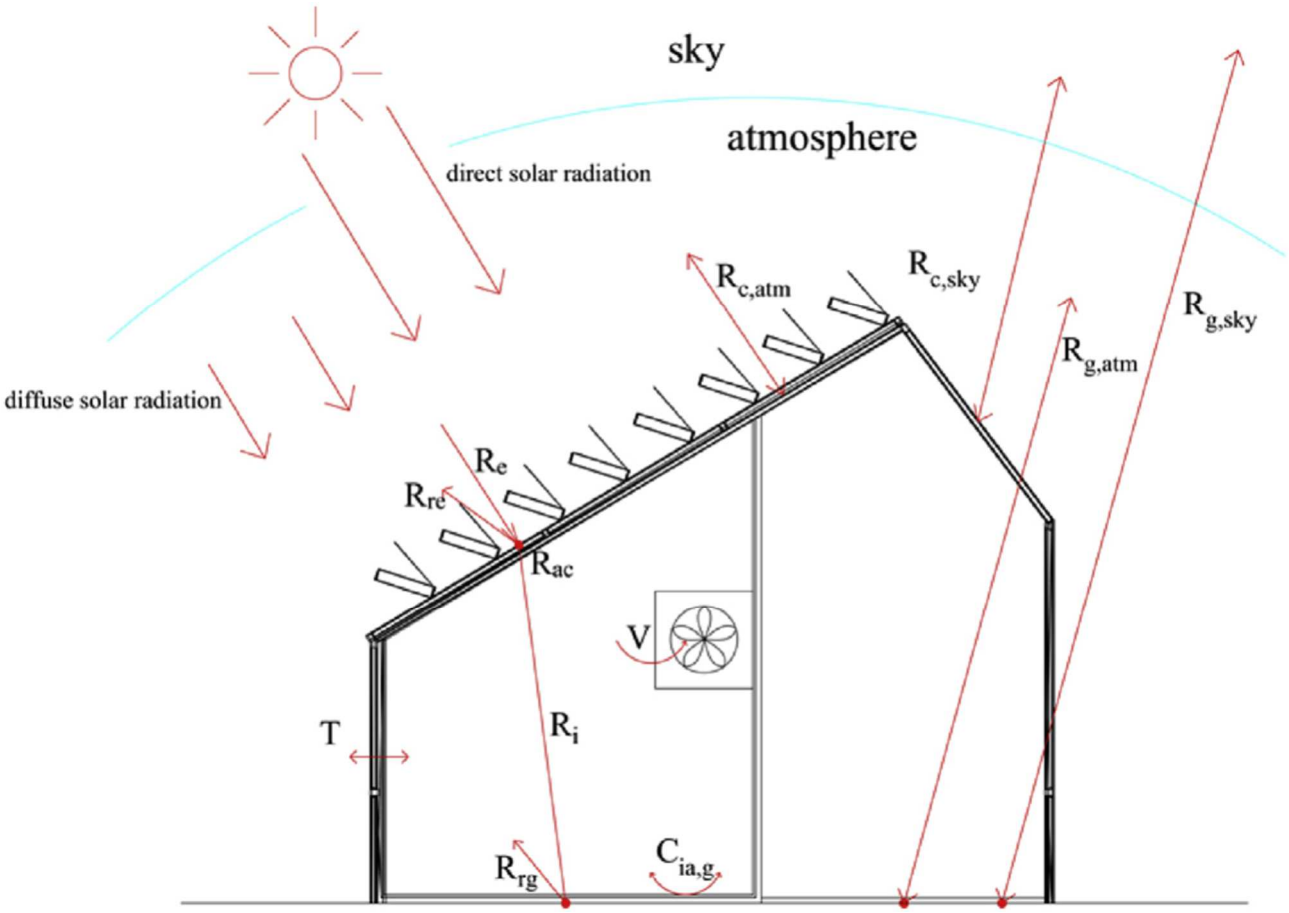

Fig. 4. Energy flows examined in the calculation of the energy balance.

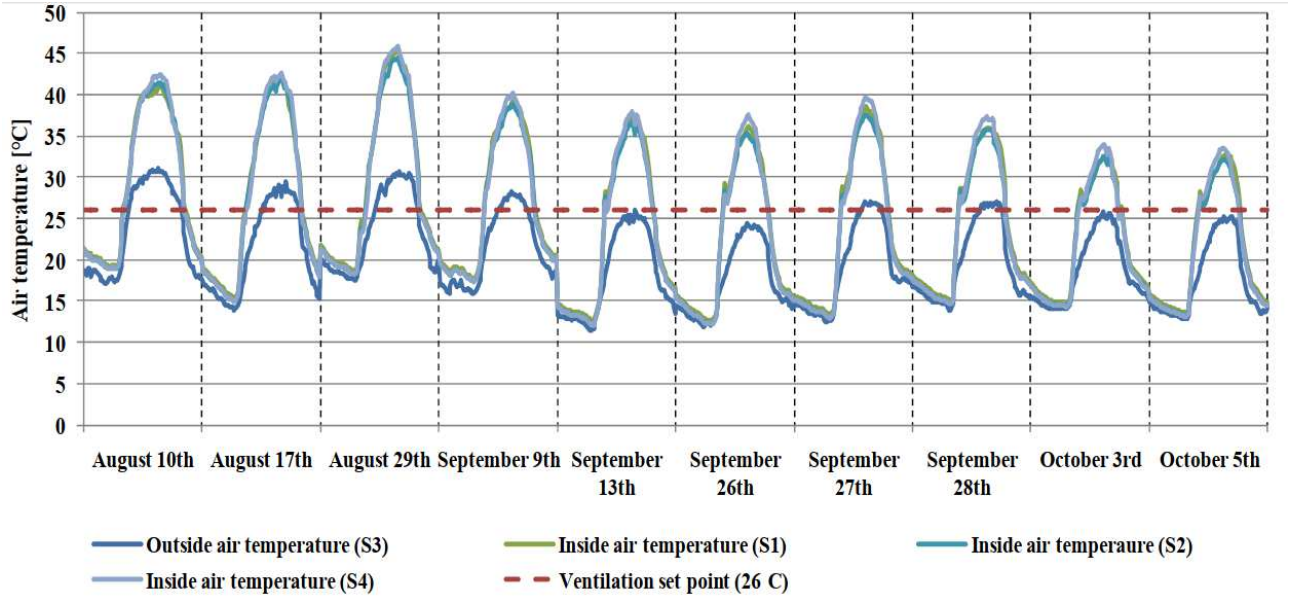

Fig. 5. Air temperatures inside and outside the greenhouse with the ventilation set point.

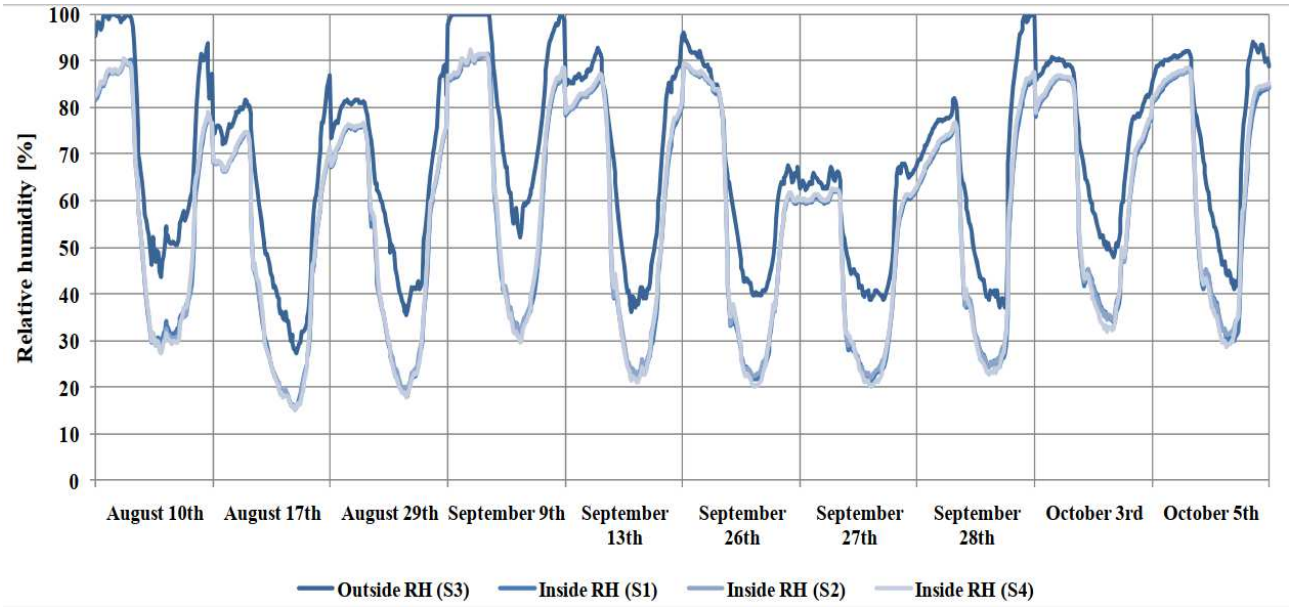

Fig. 6. Relative humidity inside and outside the greenhouse.

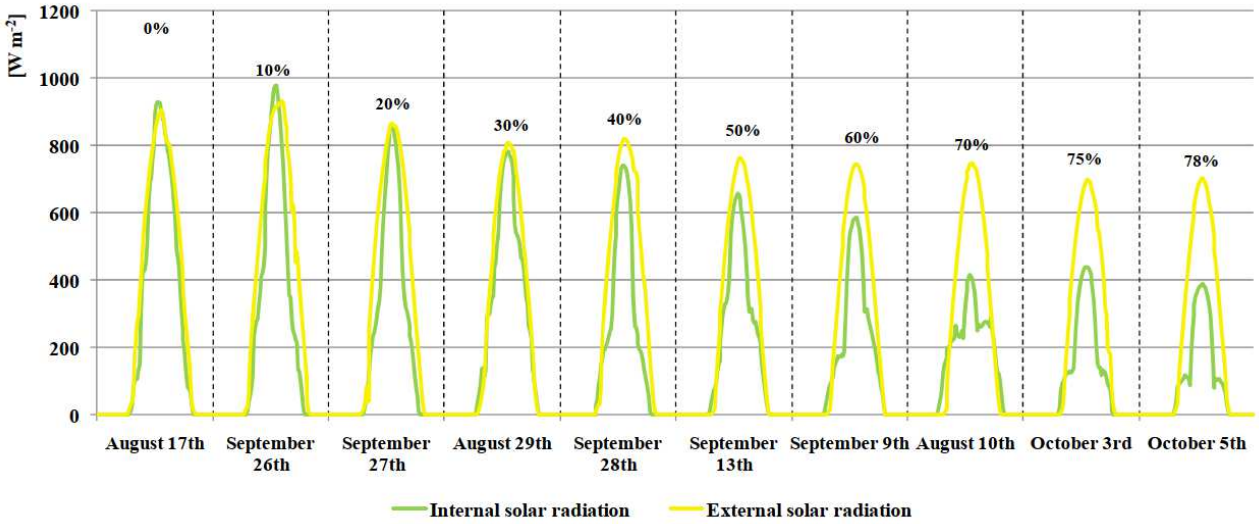

Fig. 7. Trends in the intensity of global solar radiation on a horizontal plane inside and outside the greenhouse.

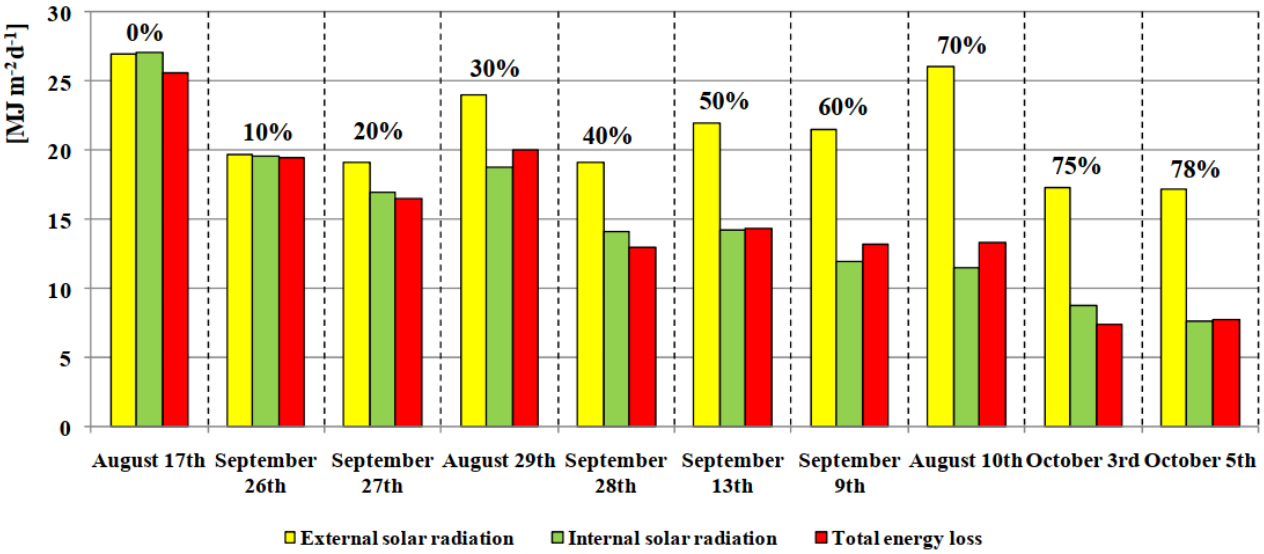

Fig. 8. Solar radiation inside and outside and the total energy losses (ventilation, radiation and transmission) from the greenhouse.

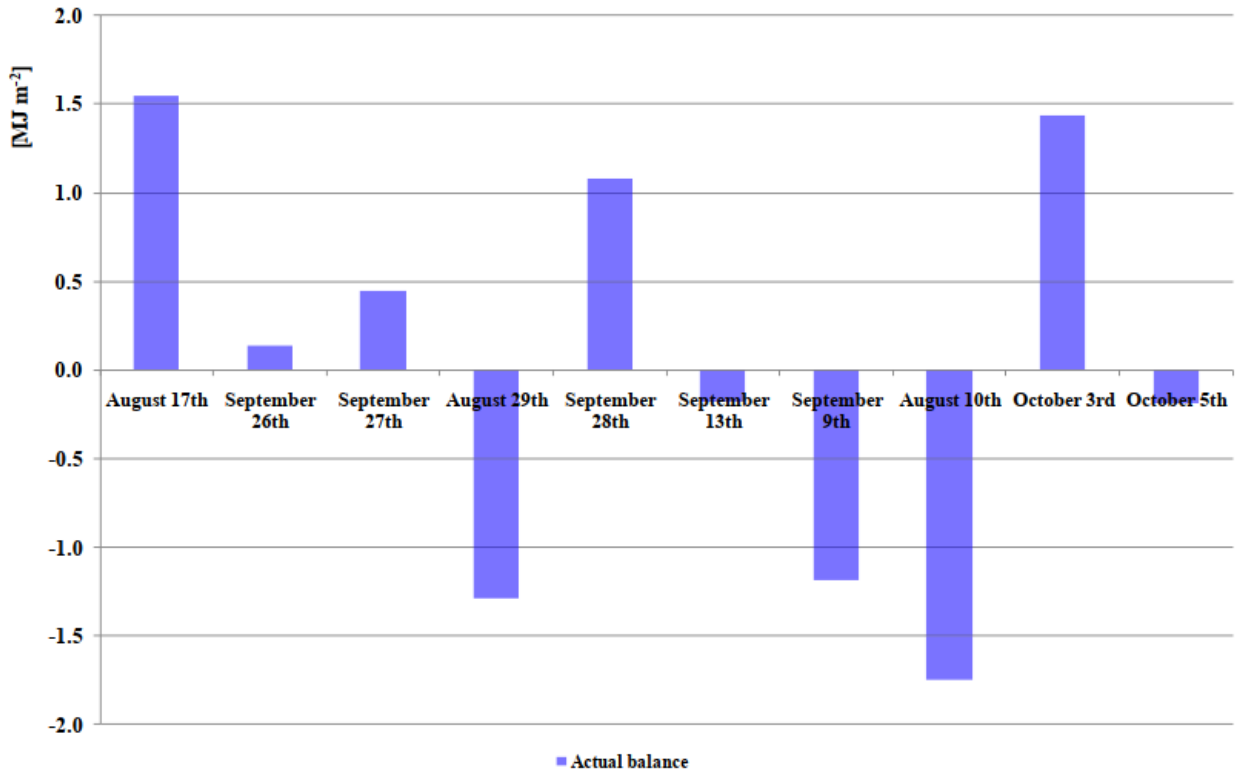

Fig. 9. Actual energy balance.

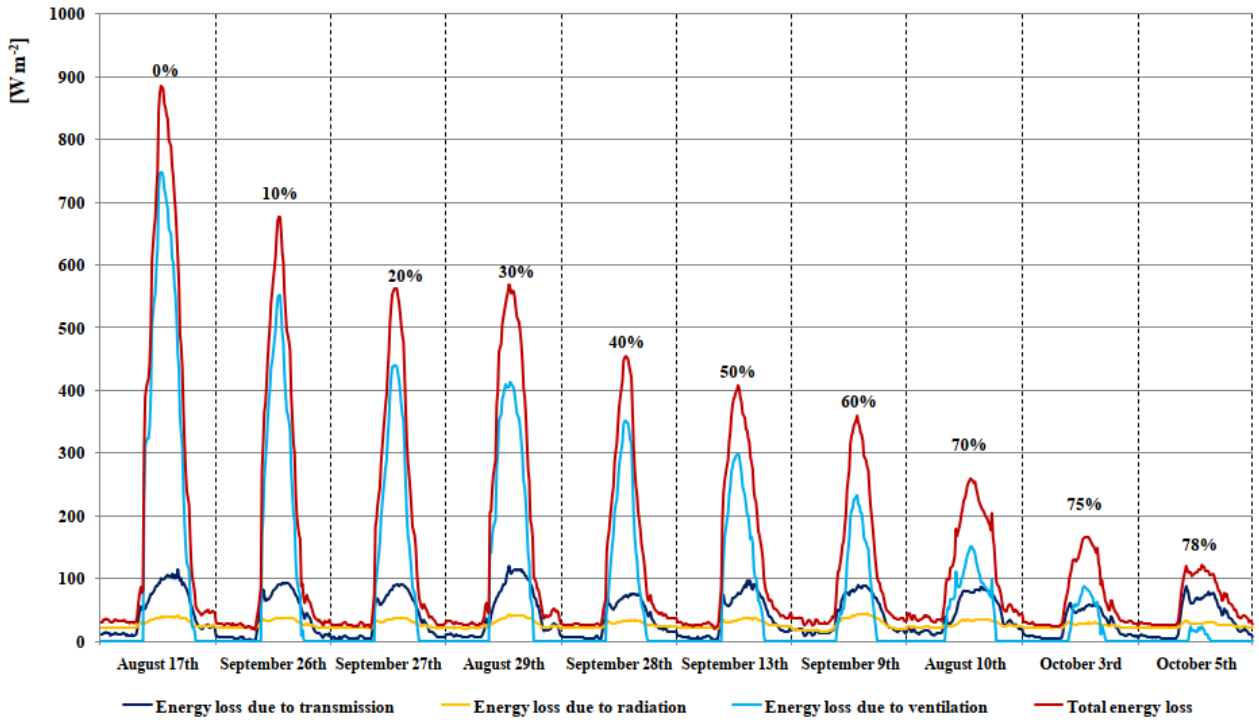

Fig. 10. Total energy losses and the trends for losses of individual energy flows (transmission, radiation and ventilation).

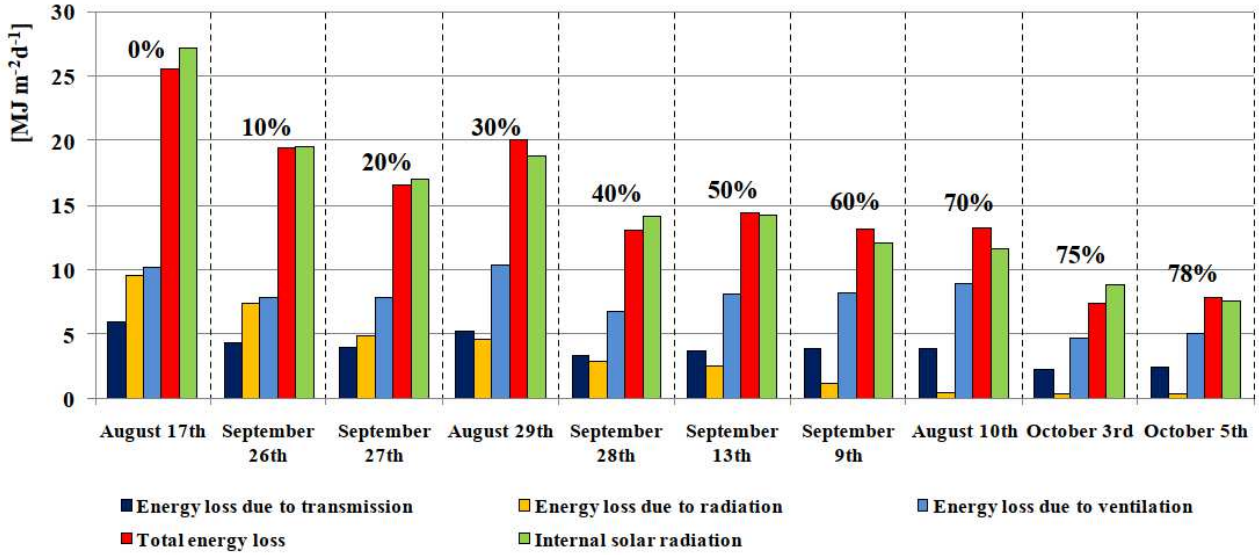

Fig. 11. Total energy lost and the loss from individual components.

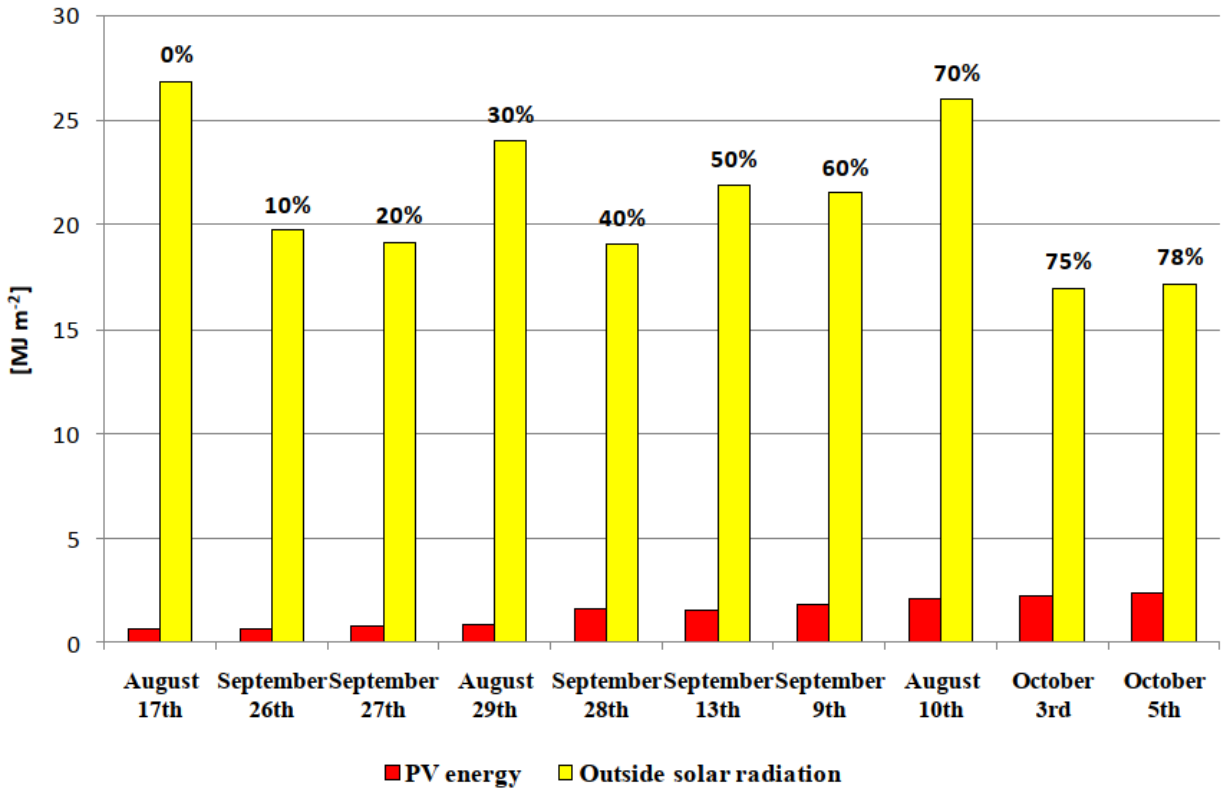

Fig. 12. Photovoltaic energy production and outside solar radiation.